Author/s:
Sabatini, RP;Zhang, B;Gupta, A;Leoni, J;Wong, WWH;Lakhwani, G

Title:
Molecularly isolated perylene diimides enable both strong exciton-photon coupling and high photoluminescence quantum yield

Date:
2019-03-14

Citation:
Sabatini, R. P., Zhang, B., Gupta, A., Leoni, J., Wong, W. W. H. & Lakhwani, G. (2019). Molecularly isolated perylene diimides enable both strong exciton-photon coupling and high photoluminescence quantum yield. Journal of Materials Chemistry C, 7 (10), pp.2954-2960. https://doi.org/10.1039/c9tc00093c.

Molecularly Isolated Perylene Diimides Enable Both Strong Exciton-Photon Coupling and High Photoluminescence Quantum Yield

Randy P. Sabatini,[1], Bolong Zhang[2], Akhil Gupta,[2] Julien Leoni[1], Wallace W.H. Wong[2], Girish Lakhwani[1]*

[1] ARC Centre of Excellence in Exciton Science, School of Chemistry, and The University of Sydney Nano Institute, The University of Sydney, NSW 2006, Australia

[2] ARC Centre of Excellence in Exciton Science, School of Chemistry, Bio21 Institute, The University of Melbourne, Parkville, Victoria 3010, Australia

KEYWORDS: Polariton, Strong coupling, diimide perylene, organic laser

***Email: girish.lakhwani@sydney.edu.au**

Strong coupling in organic media holds the promise of efficient room temperature polariton lasing with solution-processed materials. Currently, however, only five pure-organic materials have been shown to demonstrate polariton lasing. A major challenge is to achieve high exciton-photon coupling while maintaining high photoluminescence quantum yield. Here, we utilize a series of diimide perylene materials that possess sterically hindered substituents, dispersed within a polymer matrix. The rigid structures prevent aggregation and allow high photoluminescence quantum yield (PLQY) at large dye loadings. We

demonstrate that these systems can exhibit substantial Rabi splittings at dye loadings that yield film PLQYs of up to 85%, making these perylene derivatives promising materials for polariton lasers.

Introduction

While lasers have become ubiquitous in society,[1] higher conversion efficiencies are needed to sustain continued growths in fields such as telecommunications, diagnostics, and display technologies.[2] The primary way to increase efficiency is to lower the required input energy (i.e. lower the lasing threshold).[3, 4] Traditional lasers, however, require population inversion,[5] effectively setting an upper limit on device efficiency.

In contrast, polariton lasers only necessitate strong coupling between the exciton and cavity photon mode.[6] This allows operation at greatly reduced pumping thresholds. Both strong coupling and polariton lasing were first observed with inorganic materials,[6-8] but low exciton binding energies limited these early examples to cryogenic temperatures. While optimized GaN devices improved operation at room temperature,[9] their small Rabi splitting and requisite epitaxial growth remain a hindrance.

Organic materials, however, offer a number of advantages over traditional inorganic counterparts, including the ability to be solution-processed.[10] As organic excitons are Frenkel in nature,[11] high exciton binding energies result in polariton effects at room or elevated temperatures.[12] The high oscillator strengths of organics also enable much greater exciton-photon interactions, evidenced by the large Rabi splitting between polariton modes.[13] After the first demonstration by Lidzey *et al.* that porphyrin (*i.e.* an organic material) could exhibit strong

coupling,[14] these advantages motivated intensive research toward organic polariton devices.[12, 15-18]

Although many organic materials have exhibited strong coupling, only five of them have been shown to demonstrate polariton lasing.[19-23] Generally, the basic requirements for strong coupling are large oscillator strengths, narrow absorption linewidths, and small Stokes shifts; however, Cookson *et al.* determined that high photoluminescence quantum yields (PLQYs) are important in translating strong coupling into polariton lasing.[23, 24] They achieved polariton lasing with a polymer matrix doped with a small organic dye (Boron-dipyrromethene – BODIPY), using doping concentrations that result in a BODIPY film PLQY of ~11%.[23]

To improve performance (*e.g.* attain lower thresholds), dyes should be targeted with a directed goal to obtain greater PLQYs at high dye loading. Specifically, aggregation must be avoided, as it both lowers the PLQY as well as broadens the absorption linewidth.[24] Recently, we have reported synthesis of a series of perylene diimides that have substituents with varying degrees of steric hindrance.[25, 26] The enhanced rigidity forces molecular isolation of the dye and therefore significantly decreases aggregation while retaining the same electronic structure. This allows high dye loading (obtaining stronger coupling), while maintaining efficient photoluminescence efficiency.

In this report, we demonstrate that perylene diimides can achieve substantial Rabi splittings at dye loadings that yield film PLQYs of up to 85%. These properties make them ideal candidates for efficient polariton devices.

Results and Discussion

The dye series consists of 3 perylene diimides (Figure 1a). We adopt the nomenclature from Reference 26 and refer to the derivatives with phenyl, 3,5-di-*tert*-butylphenyl, and 4-trityl substituents on the imide positions as bPDI-2, bPDI-3, and bPDI-4, respectively. As the size of the substituents increases, they resist more strongly against π-π stacking and enforce molecular isolation of the molecules. However, solubility in host matrix and aggregation in spin-casted films remain important issues despite the bulky substituents. For initial tests, we spin-coated the dye (120 mM) dispersed in a poly(methyl methacrylate) (PMMA) solution (100 mg/mL in chlorobenzene) onto a glass slide with film thicknesses ~700 nm. The large thickness accomplishes two things. It allows multiple cavity modes to appear within the visible/NIR region of the spectrum, allowing greater tolerance for slight changes in thickness. It also increases the film absorbance $(a_0 L)$, whose square root is proportional to the Rabi splitting, according to the linear dispersion model:[27]

$$\Omega = \left(\frac{F a_0 L}{\pi} \delta_H \delta_c - \frac{(\delta_H - \delta_c)}{4} \right)^{1/2}$$

where Ω is the Rabi splitting (coupling strength), F is the finesse of the cavity, a_0 is the absorption coefficient, L is the optical cavity length, and δ_H and δ_c are the exciton and cavity linewidths, respectively.

The absorption and emission spectra of the dye-doped poly(methyl methacrylate) (PMMA) thin films are shown in Figure 1b at 120mM dye loading (see Figure S1 for lifetime traces). While each absorption spectrum shows a resolved Franck-Condon progression with several vibronic peaks, the emission spectra reveal varying levels of aggregation. Emission from bPDI-2 results exclusively from a broad band aggregate emission, consistent with the previous report.[26] bPDI-3 largely maintains its original spectral shape in both absorption and emission,

although the relative amplitudes in the vibronic emission bands change slightly. This much lessened degree of aggregation is attributed to the increased steric hindrance of the 3,5-di-*tert*-butylphenyl side groups. While bPDI-4 is even more sterically hindered, and thus should have the least aggregation, its emission spectrum is composed of both monomeric emission as well as a larger aggregate emission. We attribute this to its lower solubility in the PMMA host matrix. With both high dye loading and high PMMA concentration, the dye concentration in chlorobenzene required heating to ~100°C to solubilize the sample. Even so, a large degree of aggregation was expected in the solution before spin-coating, leading to the resulting emission spectrum. In this way, we mark bPDI-3 as the most promising material, as its structure allows both high rigidity and solubility.

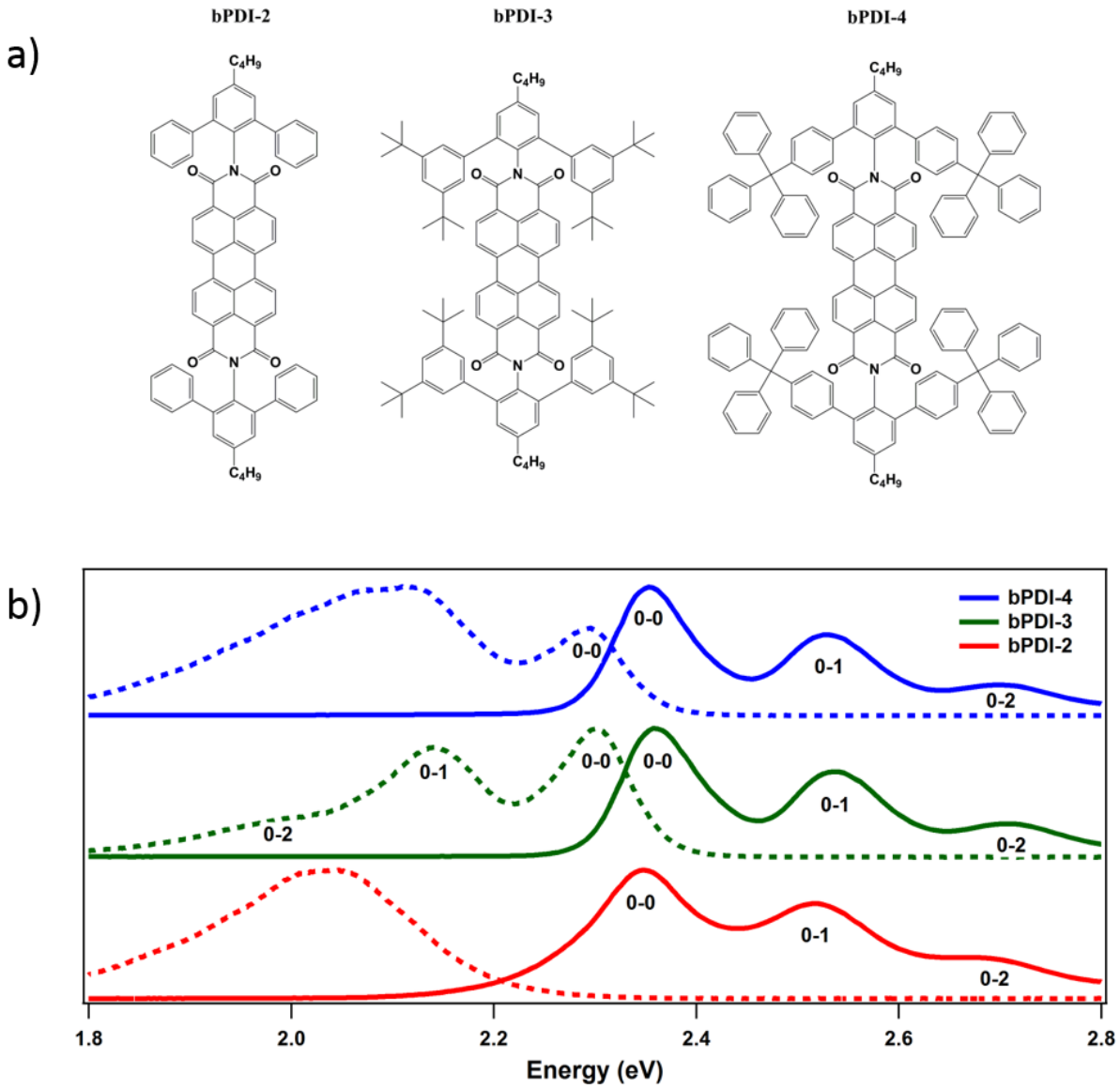

Figure 1: Sterically hindered perylenes. (a) Molecular structure of perylene, bPDI series. Rigidity increases from 2-4. (b) Absorption (solid line) and emission (dashed line) spectra of the perylene series. bPDI-3 retains the majority of its shape, but both bPDI-2 and bPDI-4 show severe signs of aggregation. The observed vibronic features are assigned.

For devices, we spin-coated the dye/PMMA solution onto a ~50 nm silver mirror; afterward, the all-metal cavity (Figure 2a) is completed with the deposition of another ~50 nm silver film on top of the active material. We first examined the transmission profile for control

devices of pure PMMA, processed by spin-coating PMMA solutions of various concentrations in chlorobenzene. The cavity resonances follow their characteristic pattern, blue-shifting as the angle of incidence is increased (Figure S2a). At 20 mg/mL, no resonance modes appear within the visible region. Mode m=1 appears for 40 mg/mL, and both m=3 and m=4 are present for 100 mg/mL (Figure S2b). The cavity thickness increases from ~100-700 nm within the PMMA concentration range (Figure S2c), and the Q-factor of the all-metal mirror cavity reaches ~20 at the greatest thickness (Figure S2d).

When the PMMA is doped with the active material, the exciton (X) and cavity (C) modes interact, and the lower and upper polariton modes (LP and UP) form (Figure 2a). Like cavity modes, polariton modes can be tracked using angle-resolved spectroscopy. We utilize angle-dependent reflection measurements to determine the peak energy for each polariton mode. Due to the vibronic structure of the perylene's absorption, the cavity mode can interact with multiple exciton modes, which can form a middle polariton (MP) mode as well. We fit the data for perylenes using the coupled oscillator model:

$$\begin{bmatrix} Ep - E & V_1 & V_2 \\ V_1 & Ex_1 - E & 0 \\ V_2 & 0 & Ex_2 - E \end{bmatrix} = 0$$

where Ep is the cavity energy (which is angle-dependent), Ex_1 and Ex_2 are the exciton energies for X_1 and X_2, respectively, and V_1 and V_2 are related to the coupling strength, or Rabi splitting (Ω) by $2V \approx \Omega$. Note that X_1 and X_2 are two vibronic peaks within the same electronic transition ($S_0 \rightarrow S_1$)

The angle-resolved data for the bPDI-2 device (120 mM dye loading) are shown in Figure 2b. The exciton and cavity modes (in this case, m=4) are represented by dashed lines; the

excitons correspond to the absorption peaks in the left inset. The resulting LP, MP, and UP reveal that the Rabi splittings for C-X_1 and C-X_2 interactions are ~100 and ~75 meV, respectively. However, the angle-dependent emission does not follow the LP. For materials to work as polariton lasers, the two states involved with emission must match the states involved with absorption (i.e. states involved with Rabi oscillations). For bPDI-2, excitation results in rapid transfer to an aggregate excited state. While this emission peak does couple to a different cavity mode, bPDI-2 is unlikely to be exploited for polariton lasing (similar to what was found for porphyrin).[14]

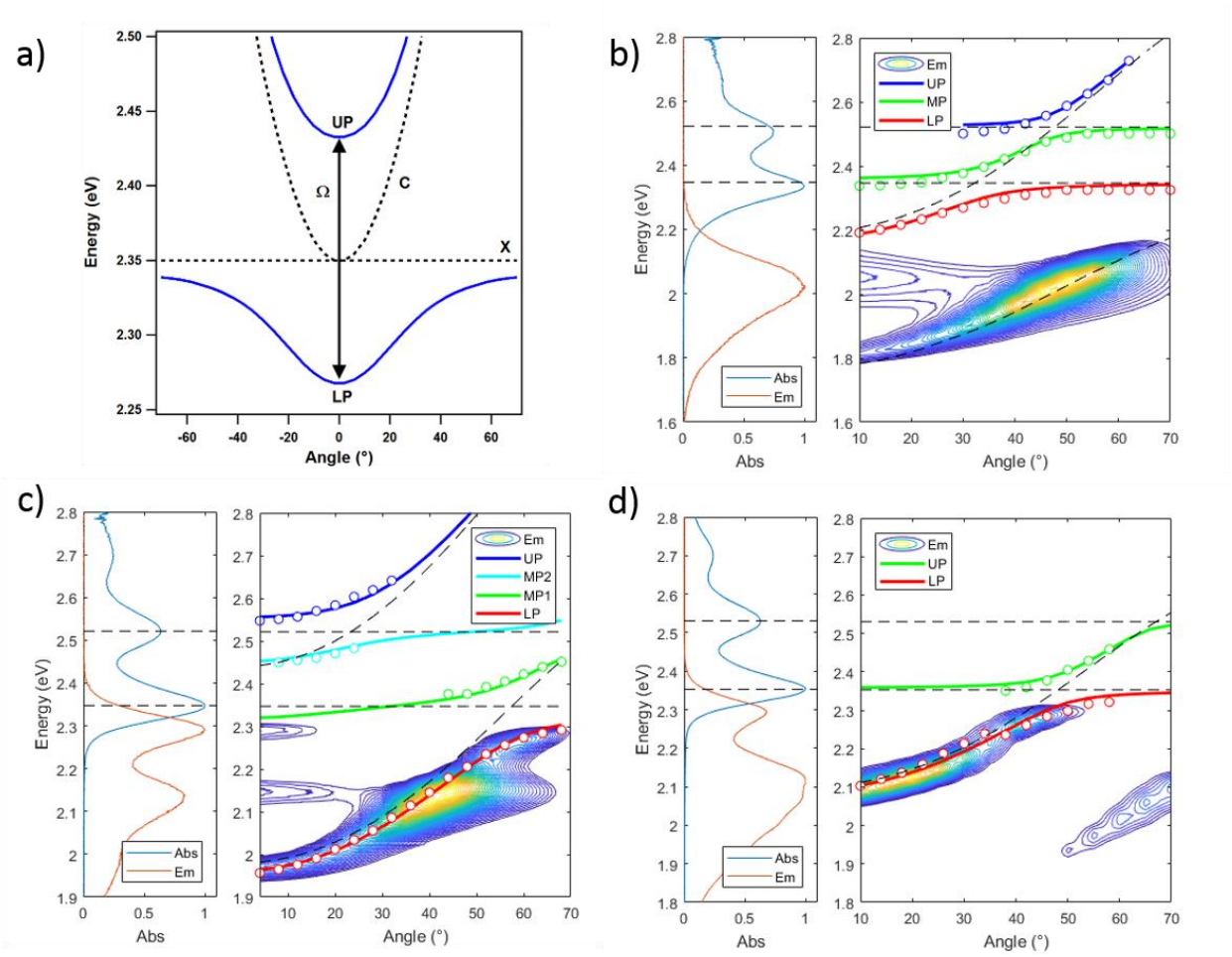

Figure 2: Strong coupling based on rigidity. (a) Schematic of polariton splitting. Polariton band energies of (b) BPDI-2, (c) bPDI-3, and (d) bPDI-4 devices based on angle-dependent reflection measurements. The coupled oscillator model was used for fits. Angle-dependent emission spectra have been overlaid on the graph. Left inset: Absorption and emission spectra of the thin film controls.

In bPDI-3 (120 mM dye loading), two cases of Rabi splitting are also seen (Figure 2c). Due to the large negative detuning, we observe the excitons interacting with different cavity modes within this angle range (i.e. X_2 interacts with C:m=5 at small angles and X_1 interacts with C:m=4 at large angles). The Rabi splittings observed are ~140 and 110 meV for Ω_1 and Ω_2, respectively. Unlike in the previous case, the main emission peak of bPDI-3 follows the LP throughout its dispersion. Note that presence of smaller uncoupled emission peaks are commonly observed in these systems.[13] The combination of strong Rabi splitting and matched emission and LP makes this material an excellent candidate for polariton lasing.

Due to bPDI-4's poor solubility, we lowered the dye loading to 60 mM. While a good quality 120 mM film could be spin-coated on glass, spin-coating it on silver left a very inhomogeneous film (leading to broad polariton resonances). At 60 mM, we observe Rabi splitting on the order of 90 meV (Figure 2d). The emission tracks the LP, but the overall monomeric emission is small compared to the broad aggregate emission. Regardless of the quantum yield of the material, a large percentage of the emission would come from a state that cannot provide polariton emission, thus making it less useful for polariton applications.

From these results, bPDI-3 is clearly the most promising polariton material. Its side groups allow both high rigidity while still allowing enough solubility to enable significant doping. We therefore tested several different dye loading conditions to assess the best

combinations of PLQY and Rabi splitting. At 15 mM, no Rabi splitting is observed around either exciton resonance (Figure 3a). Instead, the cavity mode merely sweeps through the energies. At 30 mM, Rabi splitting is now observed emerging from the X_1 resonance; however, no splitting is observed about X_2 (Figure 3b). As the dye loading is increased to 60 mM, Rabi splitting about X_1 increased more dramatically, and Rabi splitting is now slightly observed about X_2 (Figure 3c). At 120 mM, Rabi splitting is clearly observed for both exciton resonances (Figure 3d). We fit these devices using the coupled oscillator model (Figure 4) and determined the Rabi splitting. Comparing the Rabi splitting to the film absorption, we observe the expected trend that Ω is proportional to $A^{1/2}$ (Figure S3).

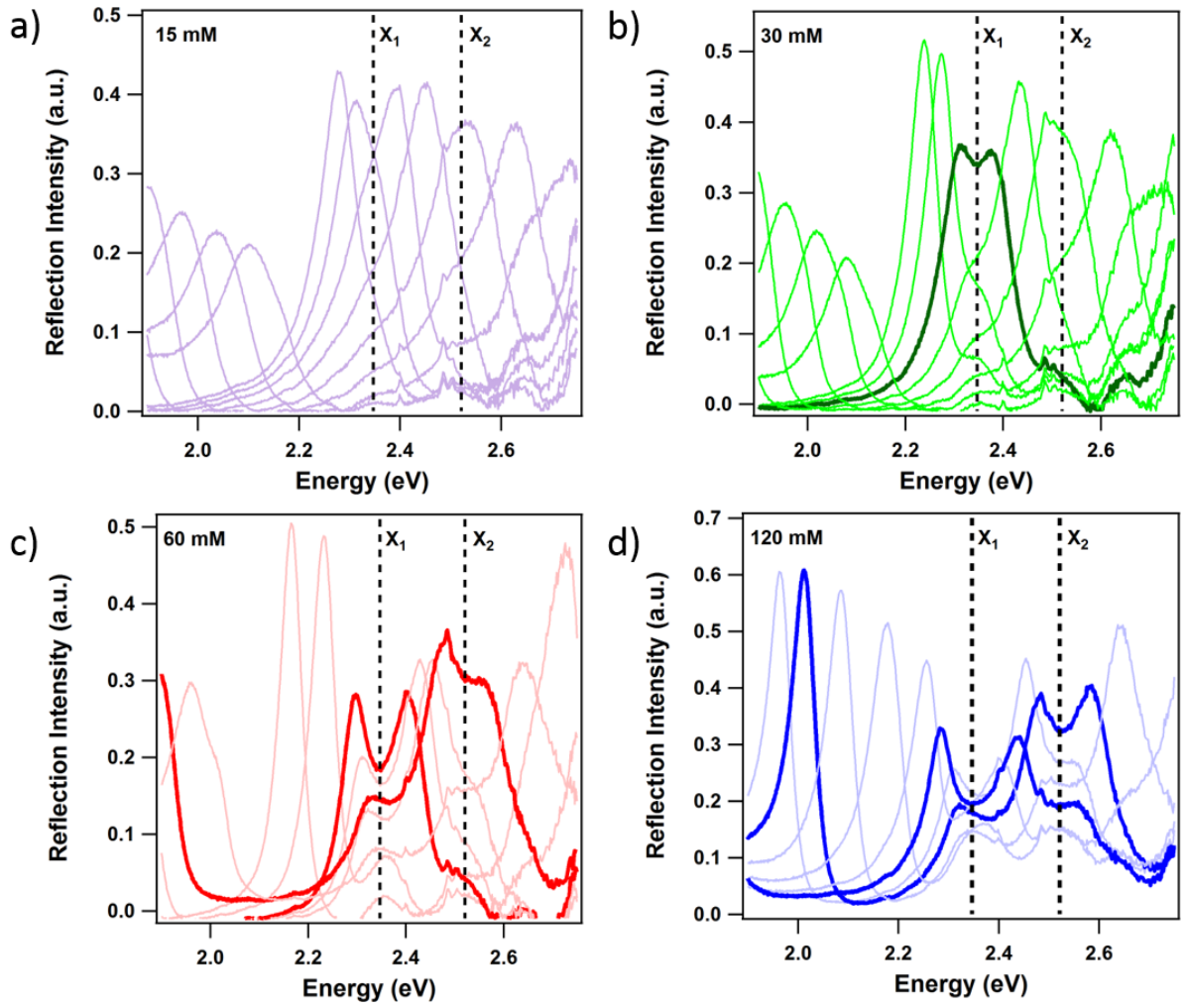

Figure 3: Dye loading effect. Angle-dependent reflection measurements of bPDI-3 at different dye loadings: (a) 15 mM, (b) 30 mM, (c) 60 mM, and (d) 120 mM. Rabi splitting becomes evident at higher dye loading. Similar spectra for bPDI-2 and bPDI-4, including Rabi splitting values for all samples, are found in Figure S4.

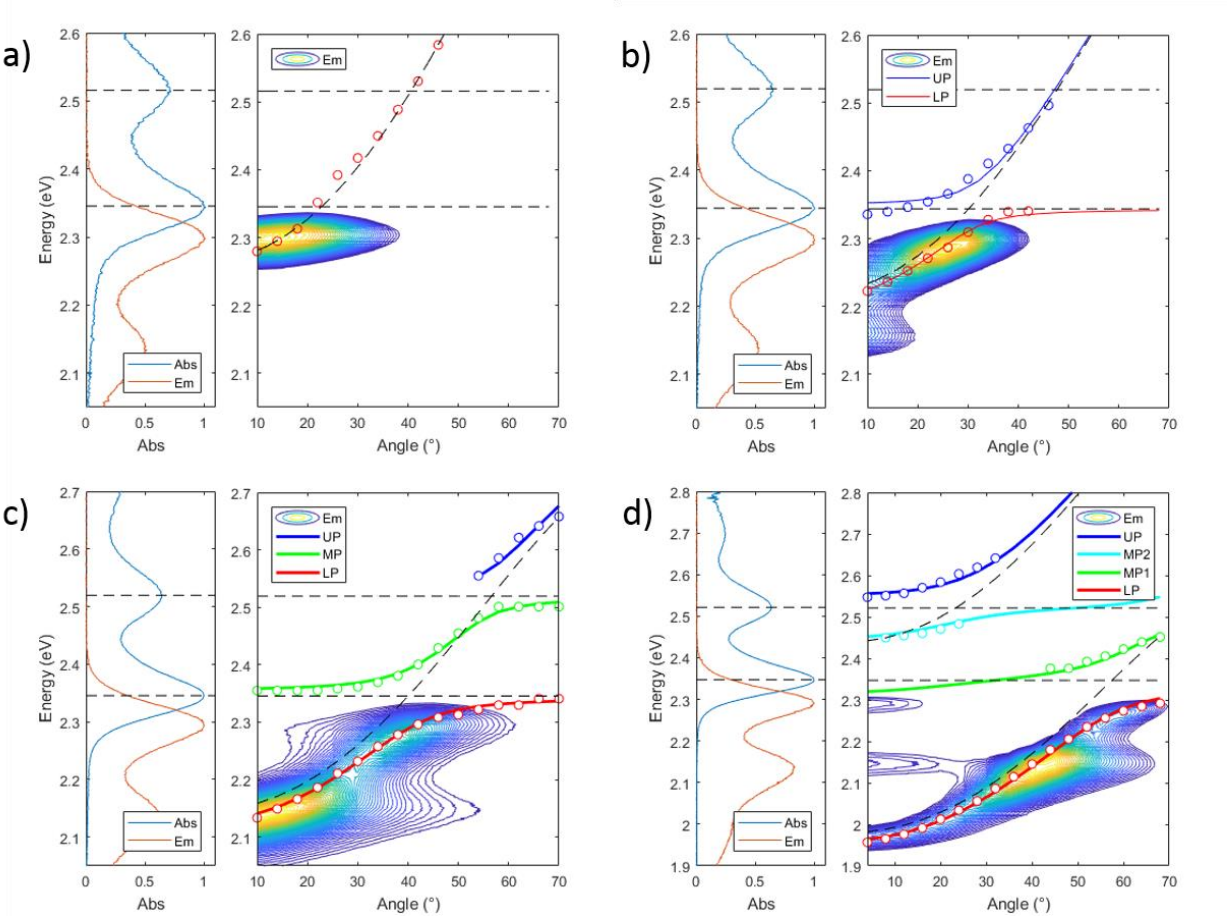

Figure 4: Rabi splitting for dye loading. Polariton band energies of bPDI-3 devices at (a) 15 mM, (b) 30 mM, (c) 60 mM, and (d) 120 mM dye loading based on angle-dependent reflection measurements. Note that the 15mM device contains no polariton bands and is in the weak coupling regime. The coupled oscillator model was used for fits. Angle-dependent emission spectra have been overlaid on the graph. Left inset: Absorption and emission spectra of the thin film controls.

These concentrations allow the positioning of bPDI-3 in the context of the field. As stated previously, only five organic materials have been shown to exhibit polariton lasing. The most recent demonstrated that this could be achieved using small molecules in a polymer matrix, even

at a modest PLQY. Here, we have utilized a sterically hindered perylene material that has similar Rabi splitting while maintaining film PLQY values above 40% (Figure 5). Furthermore, by adjusting the dye loading, we can achieve substantial Rabi splitting with film PLQY values of ~85%. Both strong coupling and high PLQY are necessary for polariton lasing. Rabi splitting is enhanced by increasing dye loading, which usually has the consequence of increased aggregation and thus diminished PLQYs. Here, however, bPDI-3 can maintain substantial PLQY even at high dye loadings, due to its rigid molecular structure. Therefore, bPDI-3 is an excellent candidate for incorporation into a high-reflectivity cavity and should exhibit polariton lasing at very low thresholds.

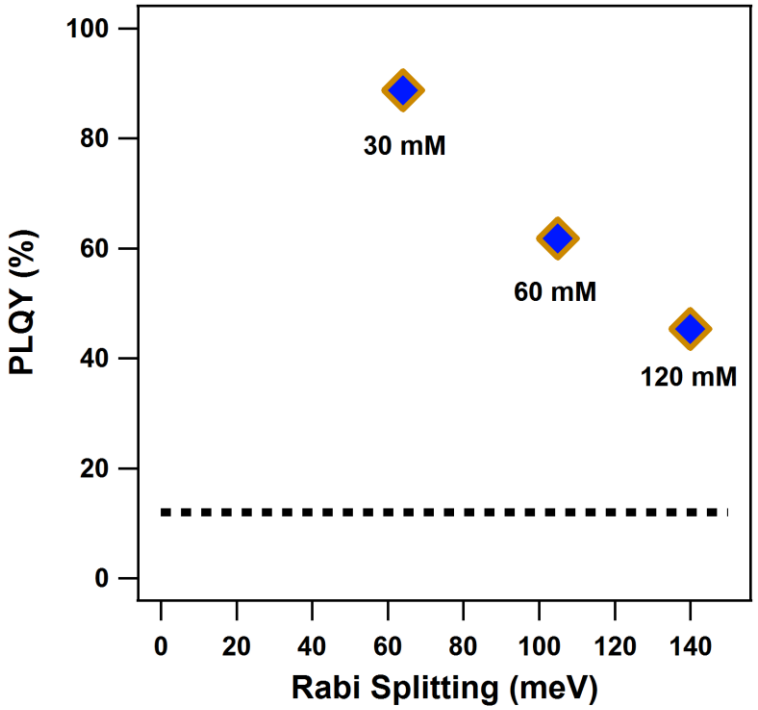

Figure 5: Outlook. Comparison of PLQY and Rabi splitting of bPDI-3 samples. PLQY data for bPDI-3 samples are taken from Reference 26. PLQY for 30 mM sample is interpolated from 20 and 40 mM samples in Reference 26. Dashed line represents lower bound of PLQY for current organic polariton lasers in literature (Table S1).

Conclusion

Few organic materials have been shown to exhibit polariton lasing, partly due to the difficulty in balancing strong Rabi splitting with high photoluminescence quantum yields. We utilize sterically hindered perylene diimide materials to minimize aggregation at high dye loadings. These perylene diimide materials exhibit substantial Rabi splittings at dye loadings that yield up to 85% PLQY in films. We show that these materials have tremendous promise as polariton lasers and expect that the high emission efficiency should translate to low lasing thresholds.

Experimental

Synthesis:

bPDI-2-4 were synthesized according to literature.[25, 26]

Film and device preparation:

For films, perylene diimides and PMMA were dissolved in chlorobenzene. Solutions of bPDI-2 and bPDI-3 were stirred and heated at 60°C for four hours; after which, they remained in solution. Solutions of bPDI-4 required heating to 100°C to solubilize the material and became cloudy again upon cooling. All solutions were then spin-coated onto glass slides.

For devices, ~50 nm of silver was deposited onto a glass slide using e-beam evaporation. Solutions of perylene diimides and PMMA were spin-coated in the same way as for films. A second ~50 nm of silver was then deposited onto the sample via e-beam evaporation to form the cavity. Film thicknesses were obtained using surface profilometry.

Optical experiments:

Absorption measurements were taken by a Cary-60 spectrophotometer. Emission measurement were made by exciting the same (NKT, Extreme) and coupling the emission sample into a fiber, before directing it to an Ocean Optics Flame spectrometer.

Angle-resolved transmission experiments were performed by sending a collimated white light source (NKT, Compact) through the sample, which was placed on a rotation stage. The white light was then collected with an integrating sphere, and the light was fiber-coupled into an Ocean Optics Flame spectrometer. Angel-resolved reflection experiments measurements were done in a similar way but with placing the integrating sphere in the path of the reflected beam.

Angle-resolved emission experiments were performed on a home-made setup where a laser source (NKT, Extreme) excited the sample. A collection lens pair swept the emission from 0-70°; emission was then coupled into an Ocean Optics Flame spectrometer.

ASSOCIATED CONTENT

Supporting Information.

The following file is available free of charge.

Lifetime decay data. PMMA control device. Rabi splitting for different dye loading. Rabi splitting versus absorbance length. Angle-dependent spectra and Rabi splitting. Literature comparison.

AUTHOR INFORMATION

Corresponding Author

*E-mail: girish.lakhwani@sydney.edu.au

Notes

The authors declare no competing financial interest.

ACKNOWLEDGEMENTS

This work was supported by the Australian Research Council Centre of Excellence in Exciton Science (funding grant number CE170100026). WWHW acknowledges support from ARC Future Fellowship Scheme (FT130100500) and support from the Australian Renewable Energy Agency which funds the project grants within the Australian Centre for Advanced Photovoltaics.

References:

1. Annual Laser Market Review & Forecast: Lasers enabling lasers, https://www.laserfocusworld.com/articles/print/volume-54/issue-01/features/annual-laser-market-review-forecast-lasers-enabling-lasers.html, (accessed January 2019).

2. N. P. Barnes, *IEEE Journal of Selected Topics in Quantum Electronics*, 2007, **13**, 435-447.

3. F. Fan, O. Voznyy, R. P. Sabatini, K. T. Bicanic, M. M. Adachi, J. R. McBride, K. R. Reid, Y.-S. Park, X. Li, A. Jain, R. Quintero-Bermudez, M. Saravanapavanantham, M. Liu, M. Korkusinski, P. Hawrylak, V. I. Klimov, S. J. Rosenthal, S. Hoogland and E. H. Sargent, *Nature*, 2017, **544**, 75.

4. A. S. D. Sandanayaka, T. Matsushima, F. Bencheikh, K. Yoshida, M. Inoue, T. Fujihara, K. Goushi, J.-C. Ribierre and C. Adachi, *Science Advances*, 2017, **3**.

5. O. Svelto, in *Principles of Lasers*, ed. D. C. Hanna, Springer, New York, 5th edn., 2010, ch. 1, pp. 1-16.

6. C. Weisbuch, M. Nishioka, A. Ishikawa and Y. Arakawa, *Physical Review Letters*, 1992, **69**, 3314-3317.

7. L. S. Dang, D. Heger, R. André, F. Bœuf and R. Romestain, *Physical Review Letters*, 1998, **81**, 3920-3923.

8. P. Senellart and J. Bloch, *Physical Review Letters*, 1999, **82**, 1233-1236.

9. S. Christopoulos, G. B. H. von Högersthal, A. J. D. Grundy, P. G. Lagoudakis, A. V. Kavokin, J. J. Baumberg, G. Christmann, R. Butté, E. Feltin, J. F. Carlin and N. Grandjean, *Physical Review Letters*, 2007, **98**, 126405.

10. M. Eslamian, *Nano-Micro Letters*, 2016, **9**, 3.

11. J. Frenkel, *Physical Review*, 1931, **37**, 17-44.

12. D. G. Lidzey, D. D. C. Bradley, T. Virgili, A. Armitage, M. S. Skolnick and S. Walker, *Physical Review Letters*, 1999, **82**, 3316-3319.

13. P. A. Hobson, W. L. Barnes, D. G. Lidzey, G. A. Gehring, D. M. Whittaker, M. S. Skolnick and S. Walker, *Applied Physics Letters*, 2002, **81**, 3519-3521.

14. D. G. Lidzey, D. D. C. Bradley, M. S. Skolnick, T. Virgili, S. Walker and D. M. Whittaker, *Nature*, 1998, **395**, 53.

15. D. G. Lidzey, D. D. C. Bradley, A. Armitage, S. Walker and M. S. Skolnick, *Science*, 2000, **288**, 1620-1623.

16. R. F. Oulton, N. Takada, J. Koe, P. N. Stavrinou and D. D. C. Bradley, *Semiconductor Science and Technology*, 2003, **18**, S419.

17. R. J. Holmes and S. R. Forrest, *Physical Review Letters*, 2004, **93**, 186404.

18. S. Kéna-Cohen, M. Davanço and S. R. Forrest, *Physical Review Letters*, 2008, **101**, 116401.

19. S. Kéna-Cohen and S. R. Forrest, *Nature Photonics*, 2010, **4**, 371.

20. J. D. Plumhof, T. Stöferle, L. Mai, U. Scherf and R. F. Mahrt, *Nature Materials*, 2013, **13**, 247.

21. K. S. Daskalakis, S. A. Maier, R. Murray and S. Kéna-Cohen, *Nature Materials*, 2014, **13**, 271.

22. C. P. Dietrich, A. Steude, L. Tropf, M. Schubert, N. M. Kronenberg, K. Ostermann, S. Höfling and M. C. Gather, *Science Advances*, 2016, **2**.

23. T. Cookson, K. Georgiou, A. Zasedatelev, T. Grant Richard, T. Virgili, M. Cavazzini, F. Galeotti, C. Clark, G. Berloff Natalia, G. Lidzey David and G. Lagoudakis Pavlos, *Advanced Optical Materials*, 2017, **5**, 1700203.

24. R. T. Grant, P. Michetti, A. J. Musser, P. Gregoire, T. Virgili, E. Vella, M. Cavazzini, K. Georgiou, F. Galeotti, C. Clark, J. Clark, C. Silva and D. G. Lidzey, *Advanced Optical Materials*, 2016, **4**, 1615-1623.

25. J. L. Banal, H. Soleimaninejad, F. M. Jradi, M. Liu, J. M. White, A. W. Blakers, M. W. Cooper, D. J. Jones, K. P. Ghiggino, S. R. Marder, T. A. Smith and W. W. H. Wong, *The Journal of Physical Chemistry C*, 2016, **120**, 12952-12958.

26. B. Zhang, H. Soleimaninejad, D. J. Jones, J. M. White, K. P. Ghiggino, T. A. Smith and W. W. H. Wong, *Chemistry of Materials*, 2017, **29**, 8395-8403.

27. Y. Zhu, D. J. Gauthier, S. E. Morin, Q. Wu, H. J. Carmichael and T. W. Mossberg, *Physical Review Letters*, 1990, **64**, 2499-2502.